

EFFECT OF HEAT TREATMENT ON THE CORROSION BEHAVIOR OF Al-10%WT Mg ALLOYS

Zermane Samira¹⁾, Chala Abdelouahed¹⁾, Belahssen Okba¹⁾*

¹⁾ *Physic Laboratory of Thin Films and Applications (LPCMA), University of Biskra, 07000, Algeria*

Received: 05.05.2017

Accepted: 03.08.2017

**Corresponding author: e-mail: belahssenokba@gmail.com, Tel.: +213 774 63 76 26, Physic Laboratory of Thin Films and Applications (LPCMA), University of Biskra, 07000, Algeria*

Abstract

In the present investigation, the effect of heat treatment on the electrochemical behavior of Al-10% wt Mg alloy in 3.5% wt NaCl is studied by different electrochemical techniques such as polarization technique (Tafel plot) and electrochemical impedance spectroscopy. It has been shown that the corrosion resistant of the alloy decreased with the ageing treatment at 250 °C for 24 h. However, this latter increased with naturally ageing. The SEM (electron microscope) and Energy Dispersive EDS characterization have shown that the alloy with the two treatments of ageing became susceptible to the pitting corrosion.

Keywords: Al-Mg alloy; ageing treatment; corrosion; microstructure

1 Introduction

The addition of selected elements to pure aluminum enhances its; mechanical, physical, and chemical properties. The addition of magnesium to aluminium gives good hardness, good weldability and favorable corrosion resistance. Alloys in which magnesium is the primary alloying element are used in ship hulls, passage boards and other products exposed to marine environments because of their excellent corrosion resistance [1,2]. Non-heat treatable Al-Mg alloys (5xxx series) have better formability but; on the other hand, they are not precipitation hardenable, and that may limit their use in certain areas, and heat treatment provides alloys with interesting physical and mechanical properties [3]. Increasing the percentage of Mg in the aluminium matrix gives an alloy with good hardness, but very susceptible to intergranular corrosion and stress corrosion [2]. However, a percentage greater than 3%wt Mg in the aluminium α matrix favours the precipitation of the β (Al_3Mg_2) phase on the grain boundary and the latter is anodic with respect to the aluminium matrix and corrodes preferentially [4]. The corrosion behavior of Al-Mg alloys is controlled by the morphology and distribution of its precipitates on the grain boundary [2, 3]. It was discovered that the kind, size, and distribution of the intermetallic phases located along the grain boundaries are regarded as the main factors responsible for the susceptibility to stress corrosion cracking [5]. A thin layer of invisible oxide forms immediately when the aluminium surfaces are exposed to the atmosphere, which protects the metal from further oxidation. Therefore the alloy becomes passive. But this behaviour can be interrupted by the existence of pitting corrosion, which produces a severe problem [2, 6]. In the present work, the electrochemical behaviour of the Al-10%wtMg alloy was investigated at two different ageing treatments by means of polarisation curves, electrochemical impedance spectroscopy, characterised by SEM and EDS.

2 Experimental material and methods

The Chemical composition of the alloy used in this study is given in **Table 1**.

These samples were heat treated as follows: homogenization at 430 °C during 17 hours, followed by rapid quenching in ice water (rapid cooling). A few samples are matured at an ambient temperature (naturally ageing), and others are aged at 250 °C for 24 hours. For the metallographic characterization, and corrosion tests, samples were polished and etched with 2 mL (HF), 3 mL (HCl), 5 mL (NH₄OH) and 180 mL (H₂O). A scanning electron microscopy (FEI Quanta 200 SEM) equipped with EDS was used to examine both morphology and elemental analysis of the samples. Corrosion behaviour was studied by using electrochemical impedance spectroscopy, and Tafel extrapolation in 3.5% wt NaCl solution. The electrochemical tests are carried out using a PGZ301 potentiostat connected to a data acquisition system equipped with software (EC-LAB V10.02). The working electrode was the test sample, the counter electrode was platinum, and the reference electrode was Hg/HgO/ 1 M KOH. All the electrochemical measurements were performed under same conditions (pH = 6.5 the pH evolves freely during the experiment, after 25 minutes of immersion, freely exposed to the atmosphere and ambient temperature). The polarisation experiments were carried out using a scan rate of 1 mV/s. Electrochemical impedance spectroscopy (EIS) measurements were obtained at the open circuit potential (OCP) in a frequency range of 10 kHz–100 mHz, with an applied AC signal amplitude perturbation of 10 mV.

Table 1 Chemical composition of Al-10% wt Mg (compositions in wt %)

Elements	Al	Mg	Fe	Mn	Cu	Si	Zn	Sn	Ti
wt%	88.55	9.94	0.4	0.08	0.03	0.6	0.4	0.03	0.04

3 Results and discussion

3.1 Microstructure

Fig. 1a shows the microstructure of the alloy with ageing at room temperature. The morphology of sample exhibit a structure with pores (defects) formed during the solidification and with the various intermetallic particles, one being dark and the other is clear. The EDS analysis of two intermetallic particles separately reveals that: the first intermetallic particle (dark) is rich in Si (**Table 2**) and the other rich in Fe (**Table 3**) (see **Fig. 1a**), as related in [6]. After the corrosion test, the **Fig. 1b** shows that there is localised corrosion with the existence of the oxide layer. Examination of this sample by EDS is given in **Table 4** shows that there is a large dissolve of Mg and Al where it appears O and Cl with a large quantity, which confirms the existence of the pits. The Fe and the Si form of the cathode intermetallic particles (potential noble with respect to the aluminum matrix) can form microcells, and a localised attack of Al. The presence of the porosities on the surface of the material may be the seat of a localised attack thus reducing the resistance to corrosion of this material [7].

Table 2 The EDS analysis result of the particle 1

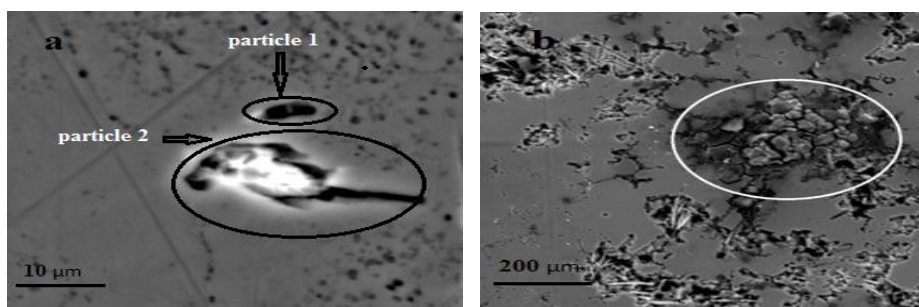
Elements	C	O	F	Mg	Al	Si
Wt%	5.30	14.84	1.75	5.05	36.58	36.47

Table 3 The EDS analysis result of the particle 2

Elements	C	O	Mg	Al	Mn	Fe	Cu
Wt%	4.36	2.37	2.31	59.08	4.21	26.87	0.80

Table 4 Chemical composition of Al-10%wtMg with ageing naturally after the corrosion test

Elements	C	O	Mg	Al	Si	Cl	Ca
Wt%	6.35	21.68	2.71	34.27	0.37	33.10	1.51

**Fig. 1** SEM micrographs of Al-10%Mg alloy with the ageing at the room temperature (a) with intermetallic particles that exist in the matrix. (b) After the corrosion test

Mizuno et al. [8], the activity of Si is zero, it can form on the Si-rich phases of the oxides of SiO₂, and the latter can prevent the cathodic reaction. Phases rich in Fe (Al₃Fe) are nobler than the matrix of aluminium, play the role of cathodes, the potential difference induces galvanic currents which translate by a localised attack on the peripheral of these phases [9]. From these results we can conclude that; the porosity has favoured the formation of the pits, so there is a high absorption of the Cl following the results of the EDS, also we can confirm that the corrosion is due to the intermetallic particles. The ageing at 250 °C is intended to have the precipitation of the equilibrium phase Al₃Mg₂. (**Fig. 2a**) shows that the precipitation of the β phase may be continuous, and also discontinuous on the grain boundaries as related by Y. Zhao et al. [10]. After the polarisation test, we notice that the corrosion is localised, and in some areas of the matrix the corrosion is intergranular, where there is the formation of pitting, **Fig. 2b** shows a layer of the oxide which covers the other uncorroded areas. The β (Al₃Mg₂) phase produces zones of localised corrosion which leads to the formation of pits in the grains and to the grain boundaries where β precipitates exist. However, **Fig. 2b** shows that the corrosion is intergranular and occurs much more on the precipitates free zones. T. Minoda et al. [11] reported that there is dissolution of the zones PFZs because of the difference between the potential of these zones PFZs and the grain wedges of the precipitates in the matrix.

3.2 Electrochemical study

3.2.1 Polarisation measurements

Fig. 3 presents the polarisation behaviour of Al-10%wtMg alloy for the two treatments ageing at room temperature and at 250°C during 24h. The cathodic polarisation curves were attributed to the water reduction, in aerated NaCl solution this reaction cause in enrichment in OH⁻ ions which cause a local increase in pH [12]. And the anodic polarisation curves were ascribed to the dissolution of Al, of which the corrosion current density rapidly increases with increasing anodic potential. However, the anodic side exhibits a passive region, where the corrosion current density increases slowly with increasing anodic potential, so on this anodic curve there are two breakdowns potential, Corrosion potential (more active), and pitting corrosion (more noble) **Tab. 5**. [13]. The corrosion potential E_c , corrosion current density i_c , and corrosion resistance

R_c , were calculated from Tafel extrapolation and presented in **Tab. 5**. The results show the ageing at 250°C during 24 h did not improve the corrosion resistance of the alloy, and the anodic

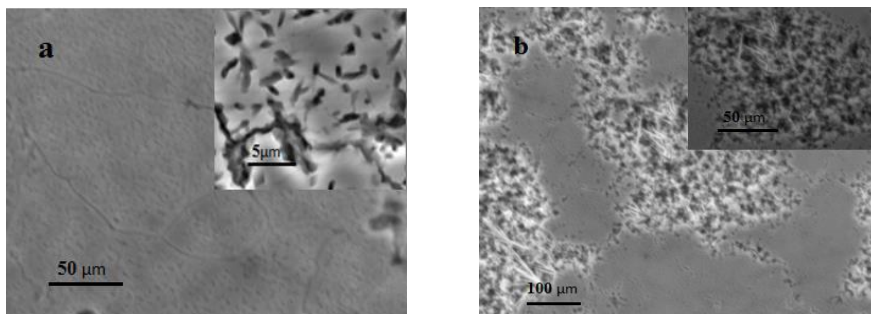


Fig. 2 Microstructures observations of the Al-10%Mg alloy with the ageing at 250 °C for 24, (a): before and, (b): after corrosion testing

current density is higher, but the ageing at room temperature leads to an increase in the corrosion resistance of the alloy with lowest current density. On the other hand, for the alloy with ageing at 250°C, the corrosion potential became noble, and the Epit (pits potential) shifts towards more negative values as related by W.J. Liang et al. [14]. This observation can be explained by the presence of the anodic phase β (Al_3Mg_2) in the matrix of Al.

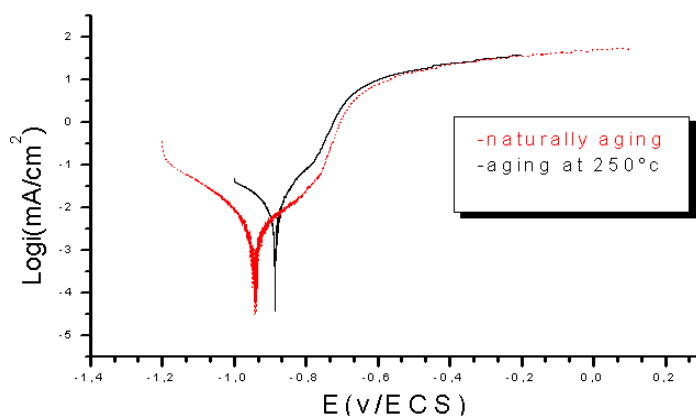


Fig. 3 Polarization curves of Al-10%Mg in a 3.5% NaCl solution

Table 5 The electrochemical parameters of the Al-10%Mg samples in a 3.5 % NaCl solution

	E_{corr} (mV)	i_{corr} ($\mu A \cdot cm^2$)	R_p (Kohm. cm^2)	Ba (mV/dec)	Bc (mV/dec)	E_p (mV)
T_{room}	-942.8	2.0409	4.41	121.7	-93.2	-757.6
250°C/24h	-885.9	9.249	2.74	88.7	-133.5	-776.7

3.3 Electrochemical impedance spectroscopy (EIS) studies

Fig. 4a presents a comparison of Nyquist responses obtained for the two treatments. The curve of the ageing at 250 °C for 24 hours has two loops; the first capacitive in the high frequency

which was related to the electrochemical reactions corresponding to the degradation of the sample. And the second inductive to the low frequencies, this is due to the phenomenon of adsorption of the reaction products on the electrode. Thus the resistance of the polarisation R_p of the system is the difference between the two diameters of two loops.

The curve EIS of ageing at room temperature exhibit one loop, a capacitive in the high-frequency region and Warburg impedance curve in the low frequency (see **Fig. 4a**). Warburg impedance is induced by the diffusion of corrosive reactants or species produced by corrosion [15]. Ageing at room temperature presents better protection. The response of the system to the frequency variations imposed may be represented by equivalent circuits. The equivalent circuit model of the corrosion system consists of the only two equivalent circuits which are shown in (**Fig. 4b**). The ageing at 250 °C during 24 h can be modelled by the equivalent circuit composed by elements: R_e represents the electrolyte resistance. R_{ct} and CPE_2 , are charge transfer resistance and pseudo double layer capacitance. L and R are respectively the inductance and resistance of the adsorbed species. And for ageing at room temperature, the equivalent circuit used includes; R_e is the electrolyte resistance

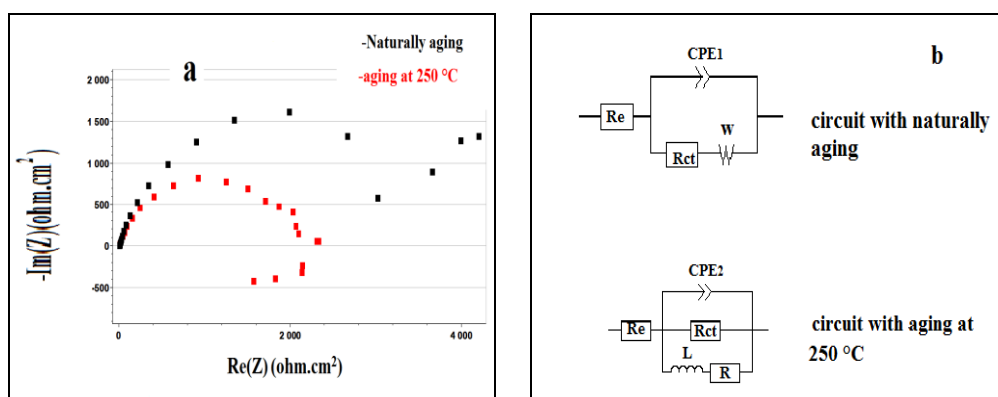


Fig. 4 (a) EIS diagram of Al-10 % wt Mg alloy in 3.5% NaCl solution, (b) Equivalent circuits which are used for modelling the EIS results

Resistance, R_{ct} characterises the charge transfer process corresponding to the dissolution reaction. CPE_1 is the pseudo double layer capacitance. The combination R_{ct} and CPE_1 is introduced to account for the presence of the surface film, and Warburg impedance (W) to account for the diffusion process. Resistance R_{ct} is the same as of the polarisation. The CPE exponent is about 0.8452 (**Tab. 6**) and 0.8393 (**Tab. 7**) for both cases indicating a deviation from the ideal capacitive behaviour. This deviation is attributed to the heterogeneous nature of the surface due to the presence of precipitates in the alloy, pitting and local defects.

Table 6 Electrochemical impedance parameters for Al-10%Mg alloy with ageing at 250 °C.

R_s (ohm)	R_{ct} (ohm)	Q ($\mu F \cdot cm^{-2} \cdot s^{a-1}$)	a	R(ohm)	L(H)
18.65	2224	40.18	0.8452	2872	66942

Table 7 Electrochemical impedance parameters for Al-10%wtMg alloy at naturally ageing.

R_e (ohm)	R_{ct} (ohm)	Q ($\mu F \cdot cm^{-2} \cdot s^{a-1}$)	a	W (ohm.s ^{1/2})
12.88	3803	24.41	0.8398	481.7

4 Conclusion

This work has studied the effect of heat treatment on the electrochemical behaviour of Al-10%wt Mg alloy; the results have been summarised as follows: electrochemical result shows a high activity of the alloy with the ageing at 250 °C, it is due to the precipitates of the β phase, which leads to the formation of pits. The inductive loop observed on the curve of impedance confirms the adsorption and penetration of chloride ions through the oxide film, and then we conclude that the ageing treatment did not improve the corrosion resistance. For the ageing at room temperature, the intermetallic particles and the porosity play a very important role in the electrochemical behaviour of the alloy. Good resistance to the corrosion, activity less important, high stability and protectiveness of the passive film are shown with the ageing at room temperature.

References

- [1] E. Ghali: Corrosion Resistance of Aluminum and Magnesium Alloys, Understanding, Performance, and Testing, first ed., Wiley, New Jersey, 2010
- [2] J.R. Davis: Corrosion of Aluminum and Aluminum Alloys, ASM International, 1999
- [3] A. Alil, M. Popovic, T. Radetic, M. Zrilic, E. Romhanji: Journal of Alloys and Compounds, Vol. 625, 2015, p. 76–84, DOI:10.1016/j.jallcom.2014.11.063
- [4] R. Goswami, G. Spanos, P.S. Pao, R.L. Holtz: Metall. Mater. Trans. Vol. 42, 2011, p. 348-35, DOI: 10.1007/s11661-010-0262
- [5] A. Zielinski. Materials Science, Vol. 34, 1998, No. 4, DOI: 10.1007/BF02360698
- [6] F. Eckermann, T. Suter, P.J. Uggowitzer, A. Afseth, P. Schmutz: Electrochim. Acta, Vol. 54, 2008, p.844-855, DOI:10.1016/j.electacta.2008.05.078
- [7] C. Vargel: Corrosion of Aluminium, eighth ed., Elsevier, Amsterdam, 2004
- [8] K. Mizuno, A. Nylund, I. Olefjord,: Corros. Sci. Vol. 43, 2001, p. 381–396, DOI: 10.1016/S0010-938X(00)00069-X
- [9] K.A. Yasakau, M.L. Zheludkevich, S.V. Lamaka, M.G.S. Ferreira: Electrochim. Acta, Vol. 52, 2007, p.7651–7659, DOI:10.1016/j.electacta.2006.12.072
- [10] Y. Zhaoe et al.: Scripta Materialia, Vol. 89, 2014, p. 49–52, DOI: org/10.1016/scriptamat.2014.07.003
- [11] T. Minoda, H. Yoshida: Metallurgical and materials transactions A. Vol. 33, 2002, p. 2891, DOI: 10.1007/s11661-002-0274-3
- [12] S. Khireche, D. Boughrara, A. Kadri, L. Hamadou, N. Benbrahim: Corrosion Science, Vol. 87, 2014, p.504–516, DOI :10.1016/j.corsci.2014.07.018
- [13] V. Guillaumin, G. Mankowski: Corrosion Science. Vol. 41, 1999, P. 421-438,
- [14] W.J.Liang, P.A. Rometsch, L.F. Cao, N. Birbilis: Corrosion science, Vol.76, 2013, p.119128, DOI:10.1016/j.corsci.2013.06.035
- [15] O. Belahssen, A. Chala, H. Ben Temam and S. Benramache: Royal Society of Chemistry RSC Advances, Vol. 4, 2014, No. 98, p. 52951-52958, DOI: 10.1039/C4RA08326A